Journal of Building Engineering 71 (2023) 106574

Contents lists available at ScienceDirect

Journal of Building Engineering

journal homepage: www.elsevier.com/locate/jobe

Experimental analysis of torsional behavior of hybrid fiber reinforced concrete beams

Mohamed Said [a], Ahmed Salah [a], Abeer Erfan [a], Ahmed Esam [b,*]

[a] Department of Civil Engineering, Faculty of Engineering at Shoubra, Benha University, Cairo, Egypt
[b] Department of Civil Engineering, Higher Institute of Engineering, Shorouk City, Cairo, Egypt

ARTICLE INFO

Keywords:
Hybrid fiber reinforced concrete beams
Carbon fiber
Steel fiber
Basalt fibers
Torsional behavior

ABSTRACT

This experimental study intended to compare the effect of hybrid fiber between carbon fiber (CF), basalt fiber (BF), and steel fiber (SF) on the torsional behavior of reinforced concrete (RC) beams. Thirteen RC beams were tested under pure torsion and loaded until failure. Beams were divided into four series: A, B, C, and D. Series A consisted of four beams: one without fibers, and others with one type of fiber (CF, BF, and SF). Each one of series B, C, and D contain two types of fibers: (CF and BF), (BF and SF), and (CF and SF) with a varying fiber content of 0.25%, 0.50%, and 0.75% in term of volume. This paper represented the results of the torsional moment, twisting angle, crack pattern, fracture modes, ductility, and energy absorption of specimens. Experiments showed that the use of a hybrid of SF and CF enhanced torsional moment, angle of twist, and energy absorption more than the hybrid of BF and CF or BF and SF. Conversely, the positive effect of the hybrid of BF and SF on ductility was greater than other hybrids. Therefore, the maximum torsional strength increased by 22.3%, 28.6%, and 65.2% when a hybrid fiber of (0.75% BF and 0.75% CF), (0.75% BF and 0.75% SF), and (0.75% CF and 0.75% SF) added, respectively. Moreover, the ultimate torsion was predicted by different theories and code provisions and a formula was developed to take the effect of hybrid fiber on the ultimate torsion of hybrid fiber reinforced concrete (HFRC) beams.

1. Introduction

Concrete demand has increased significantly over the last decades, due to the rapid and massive growth of the world construction industry. This is related to desirable concrete characteristics, such as its significant compression capacity while having a very low-tension capacity and low ductility [1,2]. Beams consider one of the structural elements that support transverse loads. Failure of a beam happens mainly because of tensile stress caused by pure shear produced by torsion. Beam torsional results may also influence structural behavior [3,4]. Thus, it is necessary to study the torsional behavior of beams.

In recent years, major advances have been made in research related to improving the behavior of reinforced concrete (RC) beams leading to the development of many effective methods and stabilization techniques to improve the torsional behavior of RC beams. Hadhood et al. [5] assessed the influence of GFRP spirals on the torsional behavior of concrete beams and found that the longitudinal and transverse GFRP reinforcement generated significant tensile stresses, which led to the evolution of the ultimate torsional moment. Kandekar and Talikoti [6] stated that the torsional strength and the angle of twist were enhanced significantly when the reinforced concrete beam was wrapped with aramid fiber. Externally bonded PBO-FRCM composite can be a suitable material for the torsional

* Corresponding author.
E-mail address: ahmed.esam@sha.edu.eg (A. Esam).

https://doi.org/10.1016/j.jobe.2023.106574
Received 5 December 2022; Received in revised form 10 April 2023; Accepted 14 April 2023
Available online 15 April 2023

strengthening of RC beams, as the torsional strength increased with increasing fiber reinforcement ratio [7,8]. Zhou et al. [9] conducted an experimental study on the torsional behavior of FRC and ECC beams reinforced with GFRP bars and found that increasing the fiber contents, enhanced the toughness and torsional strength of the beams. Besides, utilizing ferrocement U-jacketing or UHPFC jackets in wrapping sides of beams is an effective method for increasing torque carrying capacity under all states of torsion, as reported in Refs. [10,11].

Several researchers employed various types of fibers such as steel, glass, synthetic fibers, and natural fibers to improve the torsional strength, durability characteristics, and post-cracking behavior of concrete. Karimipour et al. [12] investigated the impact of SF and PPF on the torsional performance of nine RC beams. The experiments showed that the maximum torsional strength of RC beams was improved by 68.4% and 105% when 4% SF and PPF were utilized respectively. In the same line, many studies confirmed that adding steel fiber can improve the torsional strength, ductility, crack propagation, and angle of twist of RC beams [13–18]. On the other hand, Zeng et al. [19] indicated that polyethylene (PE) fibers provided sufficient bridge action in resisting crack widening at the stage of post-peak failure of load–deflection curves compared to steel fibers. Besides, Zeng et al. [20] conducted that polyethylene (PE) fibers provided a significant flexural capacity compared to steel fibers (SF), and basalt fibers (BF).

Furthermore, other researchers indicated that BF has a significant influence on improving the flexural strength, ductility, and tensile strength of concrete [21,22]. Carbon fiber is one of the most commonly employed reinforced concrete materials due to its lightweight, high strength, and great cement compatibility. So previous researchers used CF and found that the addition of carbon fibers can effectively improve the flexural and splitting strength of CFRC [23,24].

According to previous studies, using hybrid fibers in concrete provided more benefits than using a single type of fiber. Since two fibers are employed, one will improve durability and the other will enhance stiffness and strength of concrete.

Shaaban et al. [25] examined fifteen RC beams with different hybrid fibers content of polyvinyl alcohol (PVA), and polypropylene (PP), and it was found that a combination of hybrid fibers (0.75% PVA and 0.75% PP) and stirrups reinforcement (7.5 Ø 6/m) achieved adequate shear behavior, prevented sudden failure, and improved the ductility. Saravanakumar et al. [26] carried out an experimental study to measure the torsional behavior of hybrid fiber reinforced concrete beams and found that a 1.5% of hybrid of steel and glass fiber increased the torsional strength by 33%. Experimentally, Shi et al. [27] investigated the mechanical properties of macro polypropylene-basalt hybrid fiber RC and found that the HFRC containing 1% macro polypropylene fibers and 0.1% basalt fibers improved initial post-cracking strength, flexural strength, and energy absorption as compared to PC. Khan et al. [28] indicated that a HFRC containing 0.8% BF, 1% $CaCO_3$ whisker and 0.25% SF led to improvement of compressive pre-crack energy absorbed, compressive strength, compressive toughness index, and compressive total energy absorbed by 5.3%, 9.5%, 141%, and 152%, respectively, than of plain concrete. Besides, the hybrid fiber of steel fiber and polypropylene fiber plays an important role in enhancing the value of post-peak energy, ductility, and flexural strength of RC, as indicated in Refs. [29–32].

2. Research significance

This study surveyed the literature on experimental and numerical studies that show the brittle behavior of concrete under torsional load. Besides, highlight the important role of fibers in enhancing the mechanical properties of concrete. However, there are limited studies to measure the effect of hybrid fibers on the torsional behavior of reinforced concrete beams. Therefore, in this research, an experimental program was performed to identify the torsional behavior of hybrid fiber reinforced concrete beam. In addition to study the effect of testing variables (types of fibers, and fiber content) on the structural response parameters.

3. Materials properties

To manufacture hybrid fiber reinforced concrete (HFRC), CF, BF, and SF were used, Fig. 1. The detailed shape and dimensions of steel fibers are shown in Fig. 2. Besides, the properties of fibers were provided in Table 1. In this study, fibers were added to concrete mixes at 0%, 0.25%, 0.50%, and 0.75% by volume of concrete to enhance the properties of concrete, as shown in Table 2. CF's length and equivalent diameter were 35 mm and 0.01 mm, respectively. The length and diameter of BF were 30 mm and 0.015, respectively. Besides, the length and diameter of SF were 55 ± 2 mm and 1 ± 0.2 mm (Fig. 2), respectively. To produce the concrete specimens, ordinary Portland cement was mixed with gravel, sand, fibers, and then a solution of water and high range water reducers (HRWR) was

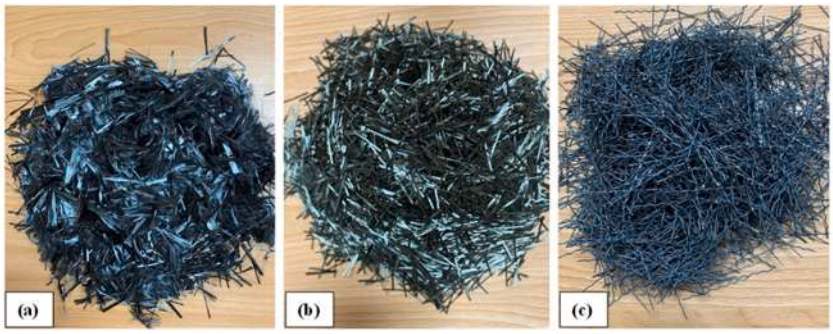

Fig. 1. (a) Carbon fiber, (b) Basalt fiber, (c) Steel fiber.

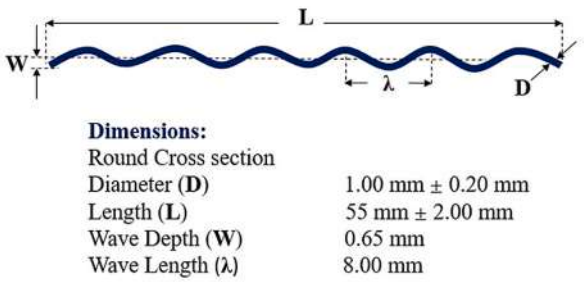

Fig. 2. The detailed shape and dimensions of steel fibers.

Table 1
Properties of fibers.

Fibers	Unit weight (kg/m^3)	Tensile strength (GPa)	Elastic modulus (GPa)	Elongation (%)
CF	1760	3.6	220	1.5
BF	2630	2.6	91	3.1
SF	7850	2.4	200	4

Table 2
Fibers content by volume of concrete.

Beams	Name of specimen	Fiber contents (by the percentage of the volume of concrete)		
		Carbon Fiber (%)	Basalt Fiber (%)	Steel Fiber (%)
B1	**Control Beams**	–	–	–
B2		0.75	–	–
B3		–	0.75	–
B4		–	–	0.75
B5	hybrid fiber (**Carbon** & **Basalt**) Reinforced concrete beams	0.25	0.25	–
B6		0.50	0.50	–
B7		0.75	0.75	–
B8	hybrid fiber (**Basalt** & **Steel**) Reinforced concrete beams	–	0.25	0.25
B9		–	0.50	0.50
B10		–	0.75	0.75
B11	hybrid fiber (**Carbon** & **Steel**) Reinforced concrete beams	0.25	–	0.25
B12		0.50	–	0.50
B13		0.75	–	0.75

added until the fibers were uniformly distributed in the mixes. The concrete mix composition was provided in Table 3. In addition, the total water/cement ratio of all mixes was kept constant at 0.44.

To estimate the compressive strength of beams, three 150 mm × 150 mm x 150 mm cubes were produced and tested. Besides, three cylinders with a diameter of 150 mm and a height of 300 mm were utilized to determine the tensile strength by splitting tensile strength test. The average concrete compressive strength after 28 days was 45 MPa and the tensile strength was 4.2 MPa. Deformed

Table 3
Concrete mixes composition.

Beams	Cement (kg)	Water (Liter)	Fine Agg. (kg)	Coarse Agg. (kg)		HRWR (Liter)	CF (kg)	BF (kg)	SF (kg)
				10 mm	20 mm				
B1	82.80	36.44	102.70	97.70	97.70	2.50	–	–	–
B2	82.80	36.44	102.70	97.70	97.70	2.50	2.22	–	–
B3	82.80	36.44	102.70	97.70	97.70	2.50	–	3.30	–
B4	82.80	36.44	102.70	97.70	97.70	2.50	–	–	9.75
B5	82.80	36.44	102.70	97.70	97.70	2.50	0.74	1.10	–
B6	82.80	36.44	102.70	97.70	97.70	2.50	1.48	2.20	–
B7	82.80	36.44	102.70	97.70	97.70	2.50	2.22	3.30	–
B8	82.80	36.44	102.70	97.70	97.70	2.50	–	1.10	3.25
B9	82.80	36.44	102.70	97.70	97.70	2.50	–	2.20	6.50
B10	82.80	36.44	102.70	97.70	97.70	2.50	–	3.30	9.75
B11	82.80	36.44	102.70	97.70	97.70	2.50	0.74	–	3.25
B12	82.80	36.44	102.70	97.70	97.70	2.50	1.48	–	6.50
B13	82.80	36.44	102.70	97.70	97.70	2.50	2.22	–	9.75

high tensile steel bars of 8, 10, 12, and 16 mm diameter were used. Table 4 showed the results of yield and ultimate strengths of the used steel bars.

4. Geometric characteristics of specimens

To produce specimens, 10 mm, 12 mm, and 16 mm diameter deformed rebars were utilized for the longitudinal reinforcement and 8 mm diameter rebars were utilized as stirrups. The arrangements and geometrical characteristics of the rebars were shown in Fig. 3.

5. Casting and curing of beams

Concrete was mixed at the Higher Institute of Engineering shorouk city Laboratory. Concrete was poured into the formwork with three layers, compacting each one using electrical vibrating. The beams were left in the laboratory until stripping from the formwork after 48 h and curing started. Curing was performed by spraying water on the jute bags placed over concrete surface for a period of 28 days. Fig. 4, presented the stages of preparing the specimens.

6. Test setup and loading condition

Specimens were tested under a two-point torsional loading condition at 28 days after curing. The two-point torsion loading condition had the advantage of providing zero moment and zero shears, allowing the central portion's torsional capacity to be measured. A load cell with a capacity of 900 kN was used to apply the load. Fig. 5, depicted the test setup and loading condition of the beams. The angle of twist was estimated using a simple mechanical system consisting of steel arms installed on both sides of the beam near the support and four LVDTs, two of them under the arm to record the deflection of the end sections due to applied load. The other LVDTs were installed on the other side to check if there was any difference between the rotation of the two sides of the beam, as shown in Fig. 6. The specimens were positioned on two plate supports. The bearing plates were provided with no bond to the beam. In addition to adjusting the position of plates under the beam to allow rotation about the mid-width of the beam at the two ends. Thus, the beam only touches the bearing plates at the rotation line with no restriction or distortion as illustrated in Fig. 6. The test was conducted under displacement control conditions, and the stopping condition was set to be the failure of the specimens.

7. Results and discussion

According to Table 2, the beam specimens were classified into four groups identified A, B, C, and D depending on the fiber content. Series A consisted of four beams designated as B1, B2, B3, and B4, which were utilized as control beams: one without fibers, and others with one type of fiber (CF, BF, and SF). The second group, Series B consisted of three specimens, designated as B5, B6, and B7, which were provided with (CF and BF) with a varying fiber content of 0.25%, 0.50%, and 0.75% in terms of volume. The third group, Series C consisted of three specimens, designated as B8, B9, and B10, which were provided with (BF and SF) with a varying fiber content of 0.25%, 0.50%, and 0.75% in terms of volume. The fourth group, Series D consisted of three specimens, designated as B11, B12, and B13, which were provided with (CF and SF) with a varying fiber content of 0.25%, 0.50%, and 0.75% in terms of volume.

7.1. Torque-angle of twist

In this study, thirteen RC beams were tested under pure torsion and loaded until failure. The torque–angle of twist of the beams was presented as shown in Fig. 7. There, the maximum torsional moment of RC beams was improved significantly by increasing the content of CF and SF. This can be explained by the role of fibers in bridging cracks which increased the strength of the concrete matrix. Besides, adding fibers decreased the cracks' width, which improved transferring stress over cracks. Previous investigations [25–30] had reported similar observations on decreasing cracks' width and improving RC beams' structural behavior. Specimens with hybrid fibers of CF and SF (group D) showed greater maximum torsional moment and angle of twist than other groups.

7.1.1. Series A

As shown in Fig. 7a, SF improved the maximum torsional strength and angle of twist of the tested control beams greater than other types of fiber. The maximum torsional strength increased by 29.5% when 0.75% CF added and 53.6% when 0.75% SF added. While adding 0.75% BF reduced the maximum torsional strength by 1.8%. This could be attributed to the higher deformation and modulus of elasticity of CF and SF while BF pulled out from the concrete matrix under small torque due to the poor bonding between them.

7.1.2. Series B

As shown in Fig. 7b, the maximum torsional strength of specimen B2 which contained 0.75% CF was greater than all specimens of group B. Thus, it was conducted that adding BF reduced the torsional strength of the hybrid specimens. On the other side, B7 which

Table 4
Tensile strength of Steel bars.

Bar Diameter	Yield strength (MPa)	Ultimate strength (MPa)
8	418.60	490.90
10	465.20	530.40
12	470.80	540.50
16	440.50	528.70

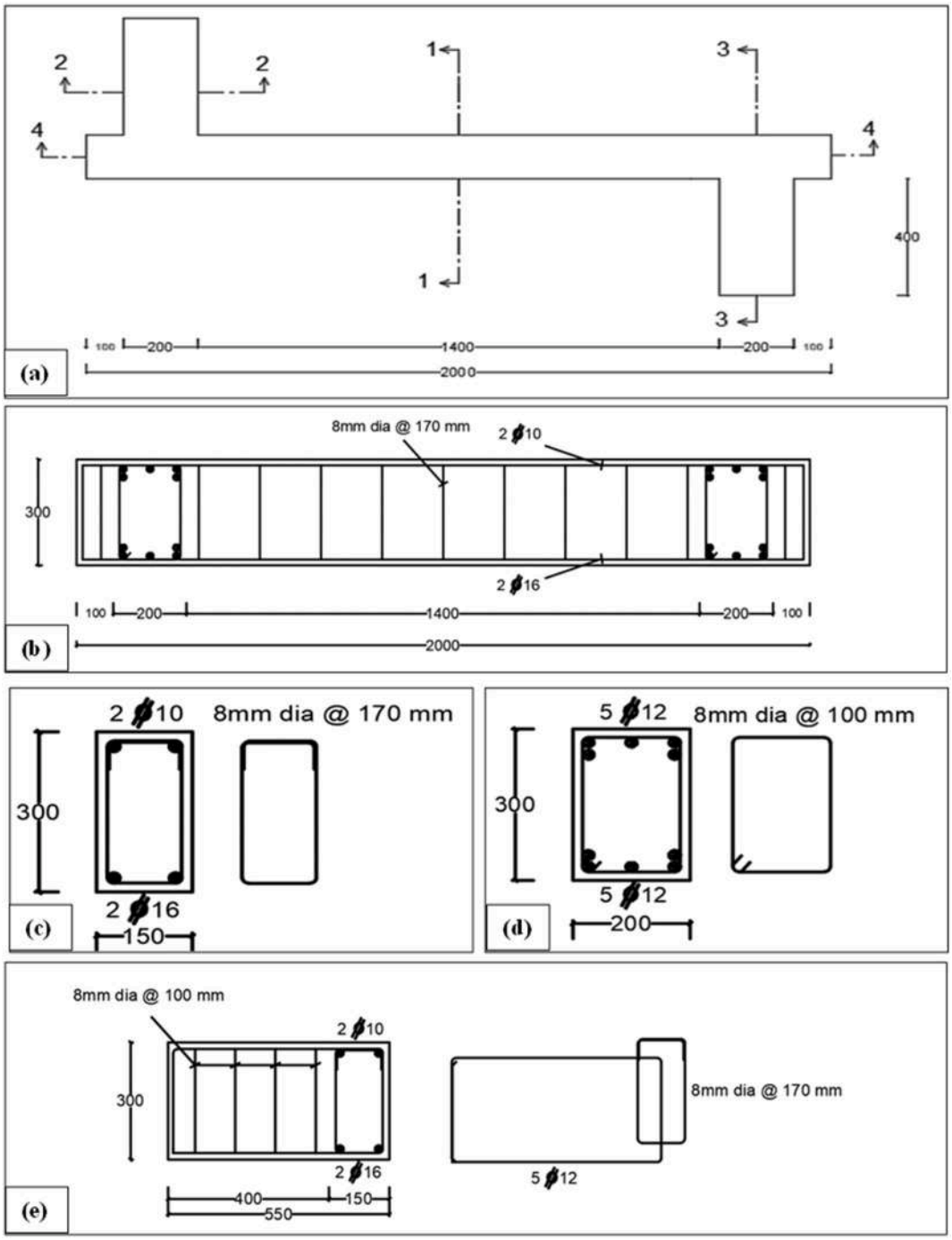

Fig. 3. Geometric properties of specimens (a) the plane of specimens, (b) longitudinal section of the beam (section 4-4), (c) cross-section area of the beam (section 1-1), (d) cross-section area of the cantilever (section 2-2) and (e) longitudinal section of the cantilever (section 3-3).

contained 0.75% BF and 0.75% CF had an angle of twist greater than other specimens. This can be explained by using the hybrid fiber of BF and CF improved the ductility of concrete more than CF alone.

7.1.3. Series C

As shown in Fig. 7c, the maximum torsional strength of specimen B4 which contained 0.75% SF was greater than all specimens of group C. Thus, it was conducted that adding BF reduced the torsional strength of the hybrid specimens as explained before. On the other side, B10 which contained 0.75% BF and 0.75% SF had an angle of twist greater than other specimens. This can be explained by

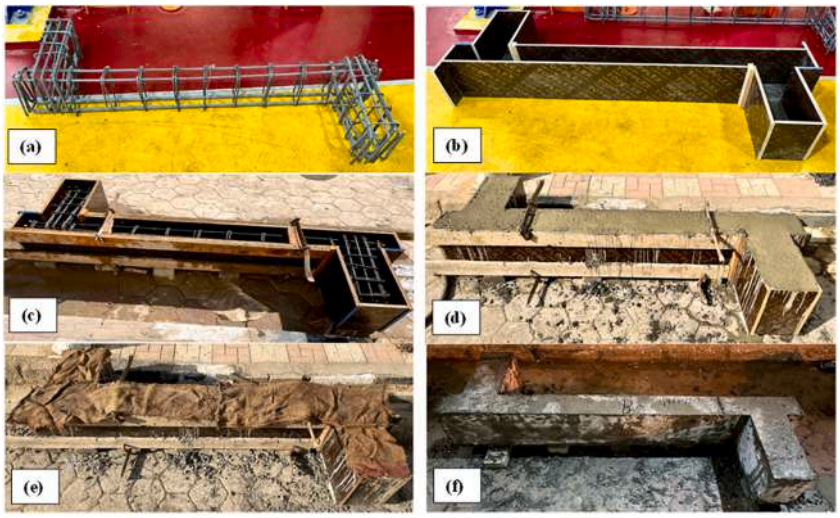

Fig. 4. Stages of preparing specimens (a) reinforcement of specimen, (b) formwork of specimen, (c) reinforcement in formwork, (d) casting specimen, (e) curing specimen by spraying water on the jute bags, (f) final specimen after curing.

using the hybrid fiber of SF and BF improved the ductility of concrete more than SF alone as they both had a high ability to stretch.

7.1.4. Series D

As shown in Fig. 7d, the maximum torsional strength of specimens was greatly enhanced by increasing hybrid fiber content. Adding hybrid fiber of (0.75% CF and 0.75% SF) increased the torsional moment strength by 7.6% than specimen B4 which contained 0.75% SF only. This can be explained by the higher deformation and modulus of elasticity of CF and SF.

In conclusion, Fig. 8, presented a summary of the influence of fibers on the maximum response of specimens. By comparing all specimens to the beam which contained no fibers we found that the addition of steel and carbon fibers to specimens B2, and B4 enhanced the torsional strength by 29.5%, and 53.6%, as well as the angle of twist was enhanced by 146.72%, and 154.92%, respectively. Therefore, adding a hybrid of them to specimens B11, B12, and B13 enhanced the ultimate torque by 34.82%, 49.11%, and 65.18%, respectively. In addition to that they enhanced the angle of twist by 269.67%, 285.25%, and 293.44%, respectively. While adding basalt fiber to specimen B3 reduced the maximum torsional strength by 1.8% but increased the ultimate angle of twist by 140.16%. Therefore, adding a hybrid of basalt fiber with steel or carbon fibers had a small effect on improving the ultimate torque and greatly enhanced the angle of twist of specimens B5, B6, B7, B8, B9, and B10 compared to group D. This can be explained by the fact that the properties of the fibers had an effective role in controlling the enhancement of the torsional strength and twisting angle of the tested specimens. There are three main properties of fibers that control the enhancement in torsional strength and angle of twist of specimens: elastic modulus, elongation, and bond of fibers with concrete. As shown in Table 2, when we compared the properties of SF, CF, and BF we found that SF had a high elastic modulus, the largest value of elongation, and the greatest ability to bond with concrete. Therefore, SF had the greatest enhancement on the ultimate torque, and angle of twist of the tested specimens. While CF came after SF in terms of strengthening the torsional strength and the angle of twist of specimens. This was because CF had the highest elastic modulus, the lowest value of elongation, and a good ability to bond with concrete. Finally, BF had a negative effect on the torsional strength of concrete and came in third place in terms of enhancing the angle of twist. This was due to BF's lowest value of elastic modulus, good elongation, and it pulled out from the concrete matrix under small torque due to the poor bonding between them.

7.2. Failure mode and crack pattern

Fig. 9, represented the specimens after failure with various fiber contents under torsional moment. Besides, the crack propagation was illustrated in this figure. There, the diagonal cracks were distributed over the length of specimens. Additionally, adding fibers improved the torsional behavior of the specimens and decreased the cracks' width. This could be explained by the role of fibers in keeping particles together in the concrete mix and improving the strength of the concrete matrix. By increasing fibers content, the cracks propagation increased throughout the specimens' length and their width decreased. Moreover, the effect of hybrid fibers in group D on decreasing cracks' width was greater than that of other groups. The reason for this higher effect could be related to their higher elastic modulus, which kept particles together in the concrete mix. Table 5, showed that the first crack torsional moment increased by 21.25%, 16.25%, and 56.25% for specimens: B7, B10, and B13, respectively. It was concluded that the hybrid fiber of CF and SF made a larger influence on first crack width than other hybrid fibers. This increment could be explained by the higher modulus of elasticity for CF and SF.

7.3. Ductility

The ductility factor, μ is an important parameter to determine the deformability of RC beams under torsional moment. It can be defined as the ratio between the failure torsional angle (θ_f) to the angle corresponding to the yield point (θ_y) [12]. Fig. 10 presented the

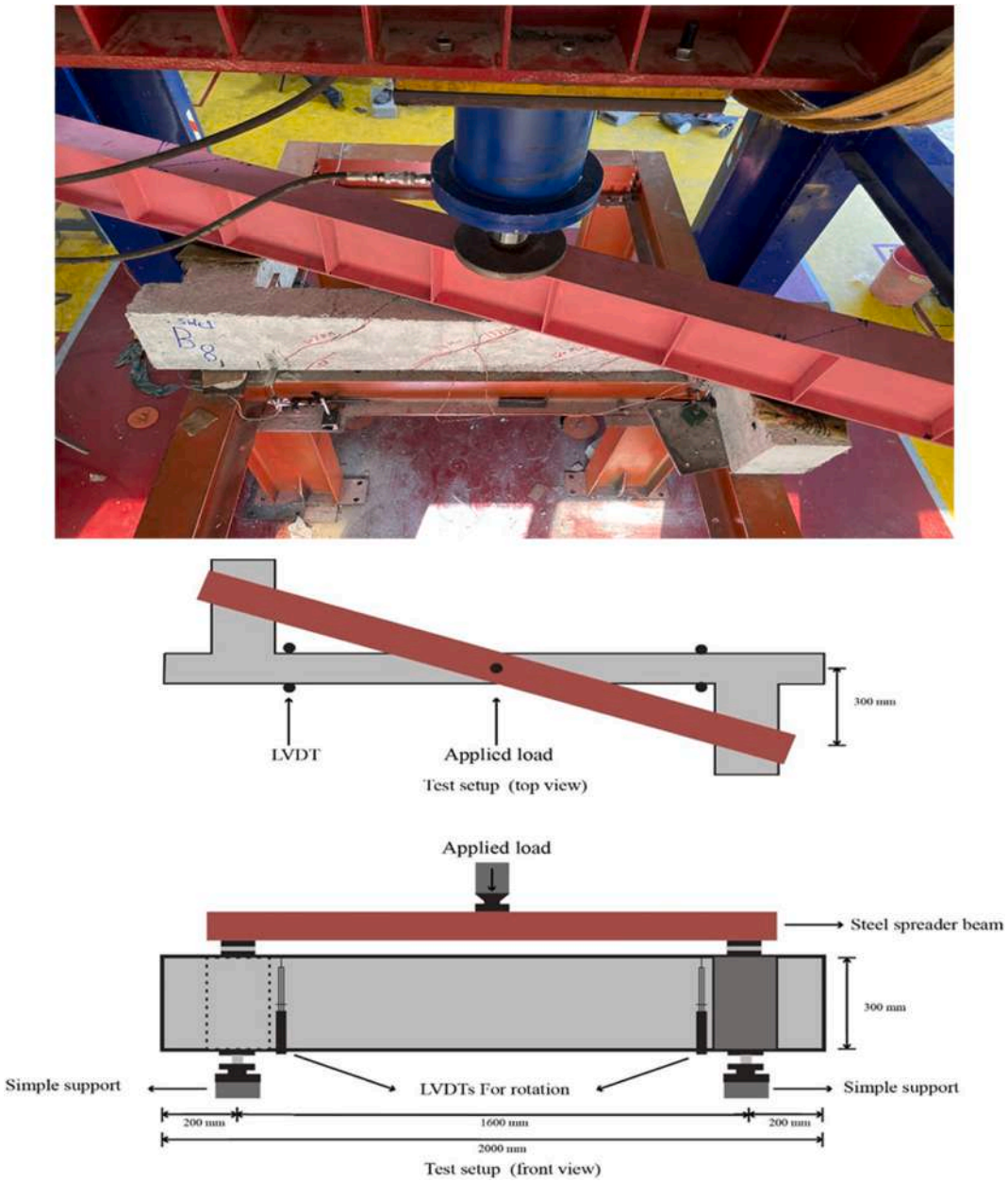

Fig. 5. Test setup and loading condition of the tested specimens.

method of determining the yield point and the angle corresponding to it (θ_y). The results of the ductility factor for specimens were shown in Fig. 11, the ductility factor of the specimens was enhanced by increasing the hybrid fiber contents. Moreover, the improvement influence of the hybrid of BF and SF on the ductility of beams was greater than that of other hybrids due to the higher deformability of BF and SF.

7.3.1. Series A

As shown in Fig. 11, SF improved the ductility of the tested control beams greater than other types of fiber. This can be attributed to the higher deformation of SF more than other types of fiber. The ductility factor increased by 55.9%, 60.4%, and 84.8% when 0.75% CF, BF, and SF were added, respectively compared to B1 which contained no fiber.

7.3.2. Series B

As shown in Fig. 11, it can be observed that adding two types of fiber improved the ductility factor more than a single type only. The ductility factor increased by 27.3%, and 37.9% in specimens B6, and B7, respectively compared to B3 which contains BF only.

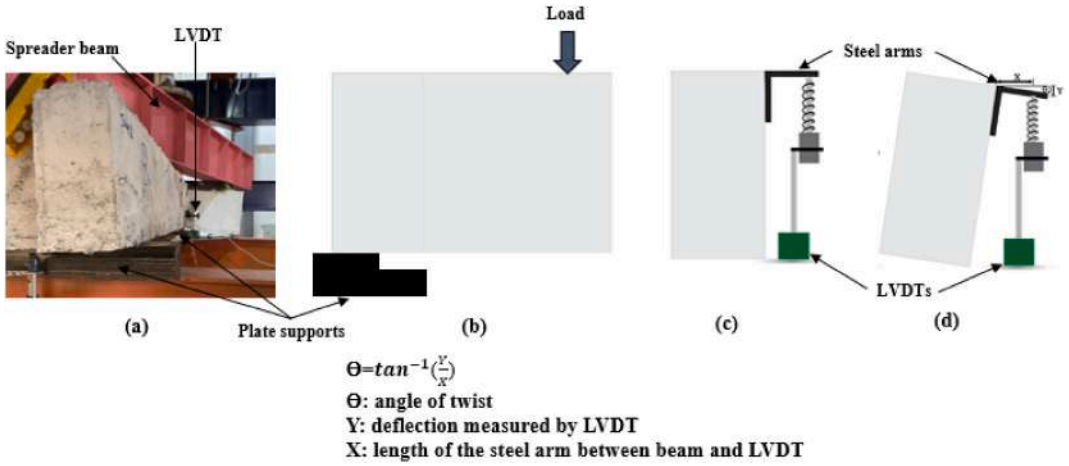

Fig. 6. Angle of twist instrumentation (a) side view of specimens, (b) cross-section area of the beam and cantilever, (c) cross-section area of the beam before loading, and (d) cross-section area of the beam after loading. **Note**: all cross sections were without steel reinforcement details.

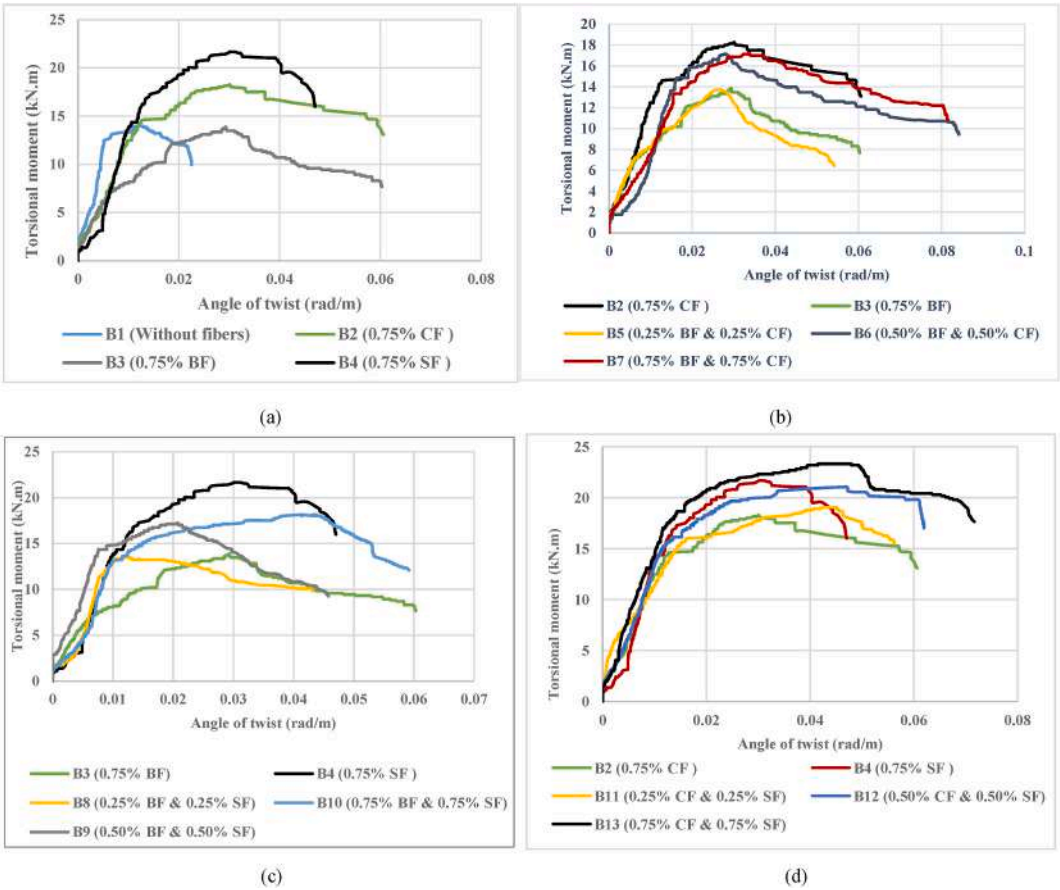

Fig. 7. Torsional moment-angle of twist relationship of specimens containing various fibers contents (a) Series A, (b) Series B compared to control beams with CF and BF only, (c) Series C compared to control beams with BF and SF only, (d) Series D compared to control beams with CF and SF only.

7.3.3. Series C

As shown in Fig. 11, The ductility factor increased by 12.2%, and 28.9% in specimens B9, and B10, respectively compared to B4 which contains SF only.

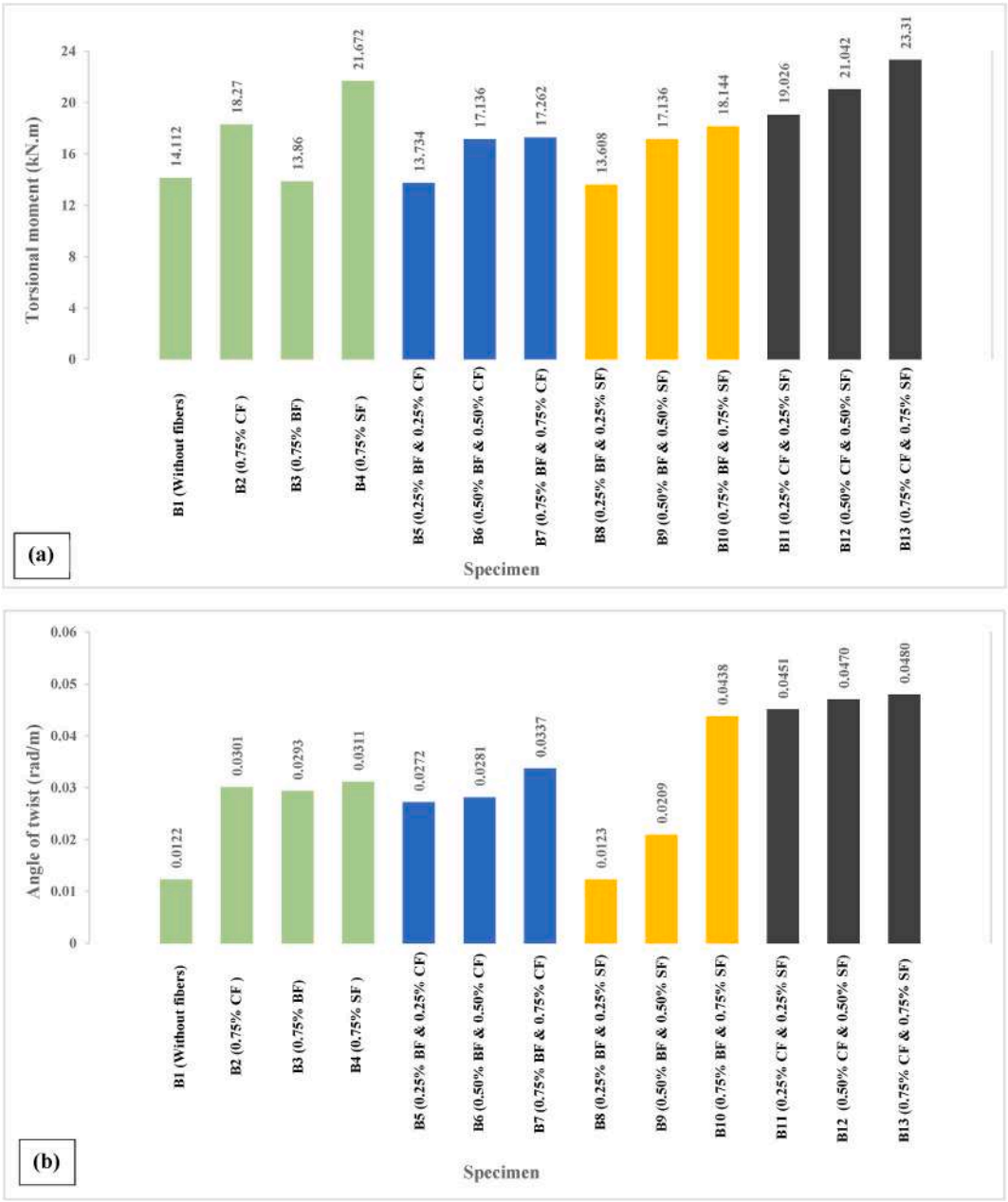

Fig. 8. Influence of fibers on the maximum response of specimens (a) maximum torsional moment (b) maximum angle of twist.

7.3.4. Series D

As shown in Fig. 11, The ductility factor increased by 11.2%, and 24.9% in specimens B12, and B13, respectively compared to B4 which contains SF only.

In conclusion, Fig. 11, presented a summary of the influence of fibers on the ductility of specimens. With comparing all specimens to the beam which contained no fibers we found that the ductility increased by 59.9%, 60.4%, 84.8%, 121.2%, 138.2%, and 130.9% in specimens B2, B3, B4, B7, B10, and B13, respectively. Results show that hybrid fibers improved the ductility of concrete with more than one type of fiber. This can be explained by increasing the hybrid fiber content played an important role in bridging micro and macro cracks which made the concrete more ductile.

7.4. Energy absorption

This study calculated energy absorption as the area under the torque angle of twist curves up to ultimate torsion [34]. Fig. 12, indicated that there was a significant increase in the energy absorbed by a deflection by adding a hybrid fiber of SF and CF more than

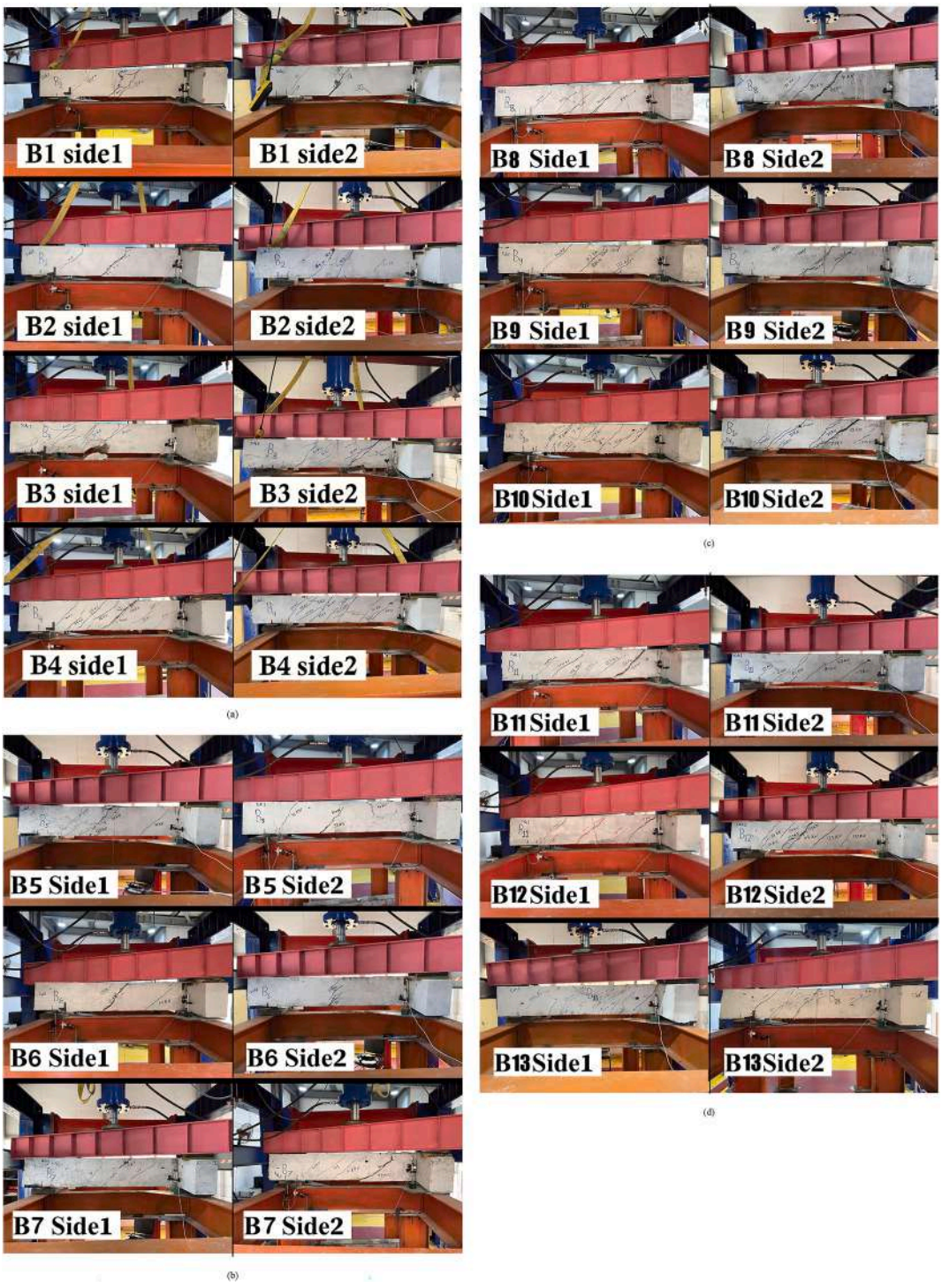

Fig. 9. Represents specimens after failure under the torsional moment, (a) series A, (b) series B, (c) series C, and (d) series (D).

other hybrids. Referring to group A results, the energy absorbed for Specimens B2, B3, and B4 increased by 225%, 133.3%, and 291.6%, respectively. Adding hybrid fiber of CF and BF (group B) had a similar effect as adding one type of them. Indicating to group C results, the energy absorbed for Specimens B9, and B10 increased by 125% and 416.7%, respectively. Series D showed a significant improvement in energy absorption compared to other groups. It increased the energy absorbed by 458.3%, 550%, and 641.7% for specimens B11, B12, and B13, respectively. This can be explained by the higher modulus of elasticity of CF and SF than BF.

Table 5
First crack load and first crack torsional moment.

Specimen	First crack load (kN)	First crack torsional moment (kN.m)
B1	80	12.00
B2	85	12.75
B3	80	12.00
B4	87	13.05
B5	80	12.00
B6	90	13.50
B7	97	14.55
B8	80	12.00
B9	88	13.20
B10	93	13.95
B11	104	15.60
B12	107	16.05
B13	125	18.75

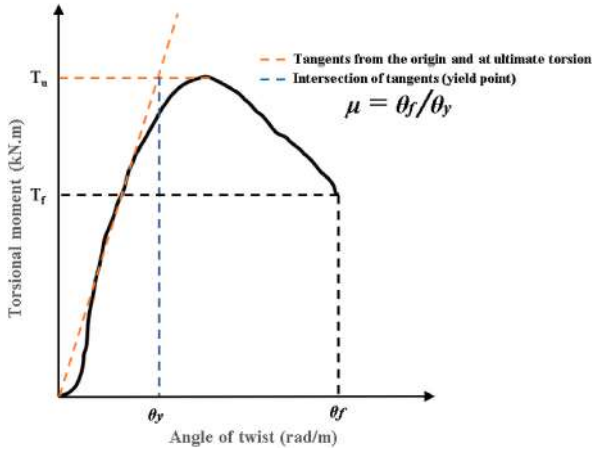

Fig. 10. Ductility factor, failure torsional angle, and the angle corresponding to the yield point [33].

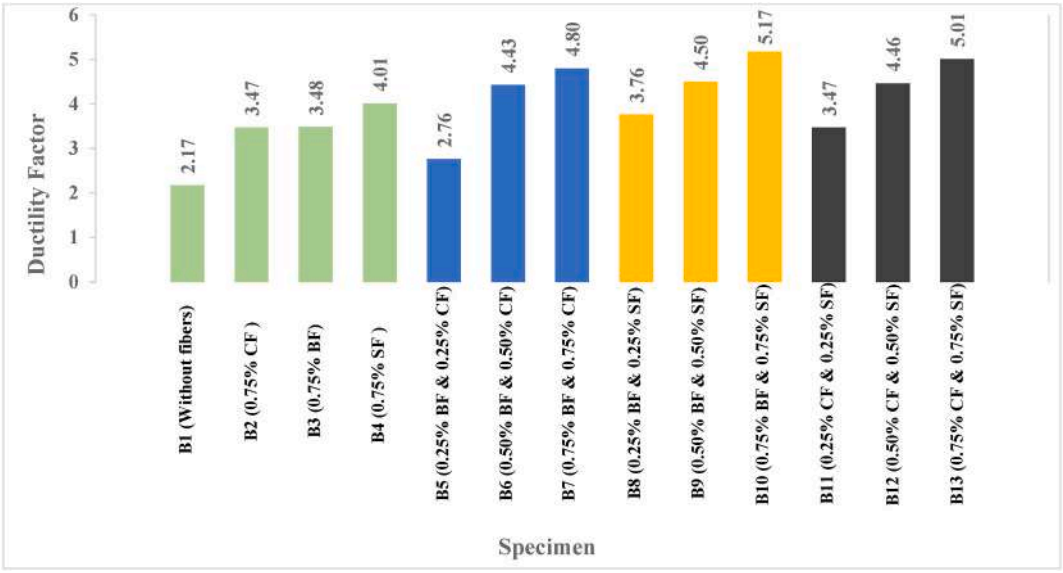

Fig. 11. Influence of fibers on the ductility of specimens.

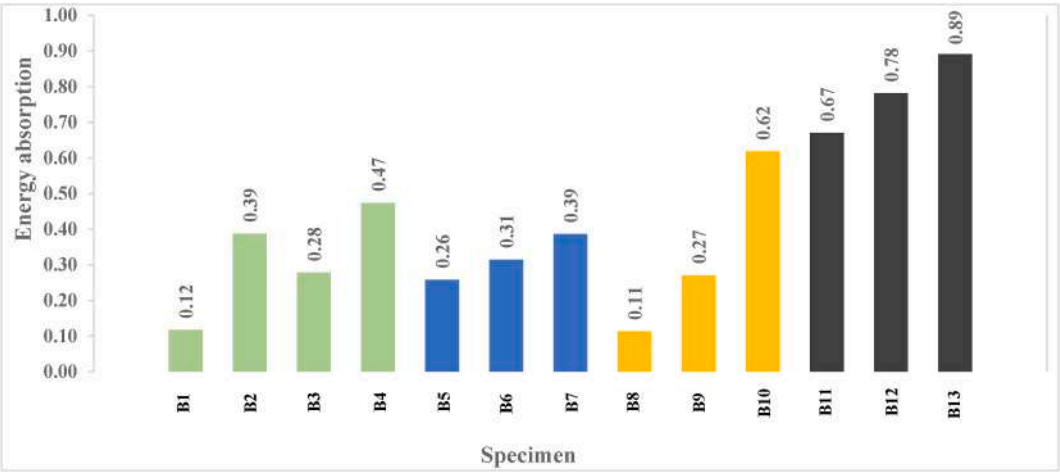

Fig. 12. Influence of fibers on the energy absorption of specimens.

7.5. Torsional stiffness

The torsional stiffness of test specimens was assessed by initial stiffness (Ki), ultimate stiffness (Ku), and stiffness degradation. Ki was estimated as the initial slope of the torsional moment–angle of twist curve. Ku can be determined through the slope of the torsional moment–angle of twist curve at 90% of maximum torsional moment. While the stiffness degradation was calculated as the ratio between ultimate stiffness (Ku) to initial stiffness (Ki).

Table 6, presented summary for initial stiffness (Ki), ultimate stiffness (Ku), and stiffness degradation ratio results. The results showed that adding hybrid fiber improved the torsional stiffness. This improvement was clearly shown in the values of stiffness degradation as shown in Fig. 13. Stiffness degradation ratio for series A increased by 97%, 75%, and 90% for B2, B3, and B4, respectively. Series B showed an increase in stiffness degradation ratio of 95%, 143%, and 203% for B5, B6, and B7, respectively. Stiffness degradation ratio for series C increased by 77%, 86%, and 192% for B8, B9, and B10, respectively. In the same line, series D showed the highest increase in stiffness degradation ratio by 126%, 185%, and 210% for B11, B12, and B13, respectively.

In conclusion, increasing the hybrid fiber content to 1.5% in specimens B7, B10, and B13 increased the stiffness degradation of specimen which improved the torsional stiffness. This could be explained by the role of fibers in bridging cracks which led to improve the torsional behavior and made it more regular.

8. Ultimate torque prediction

The internal torsional resistance arises from three sources: the stirrups' axial forces, the concrete's shear-compression force, and the longitudinal bars' dowel force. The ultimate torsional moment can be predicted by different theories and code provisions [35–39]. Table 7 presented a summary of the formulas that predicted the ultimate torsional strength and the assumption for each theory. It is fundamental to note that the selected models in this study were carefully selected based on increased popularity in the literature.

Since the ultimate torsion strength is the focal point of this study, the prediction of the five models had been utilized to estimate the ultimate torsion strength. Table 8 predicted ultimate strengths and ratios of predicted-to-experimental ultimate strength [$T_{u(pre)}/T_{u(exp)}$] for ACI 318-14 [35], GB 50010 [36], Eurocode2 [37], AS3600 [3], and Li model [39]. It could be observed that Li models' predicted values [$T_{u(pre)}$]and Eurocode2 predicted values [$T_{uL(pre)}$] (due to the longitudinal bars contribution) [37] were in good

Table 6
Initial stiffness, ultimate stiffness, and stiffness degradation.

Specimen	Initial stiffness (kN.m^2/rad)	Ultimate stiffness (kN.m^2/rad)	Stiffness degradation (%)
B1	2114.09	178.18	8.43
B2	1383.32	229.62	16.60
B3	903.40	132.90	14.71
B4	1456.72	233.23	16.01
B5	897.72	147.33	16.41
B6	866.54	177.45	20.48
B7	854.24	218.18	25.54
B8	2071.17	308.74	14.91
B9	1891.41	296.30	15.67
B10	873.06	214.85	24.61
B11	1274.64	242.50	19.02
B12	1340.38	322.44	24.06
B13	1368.45	358.04	26.16

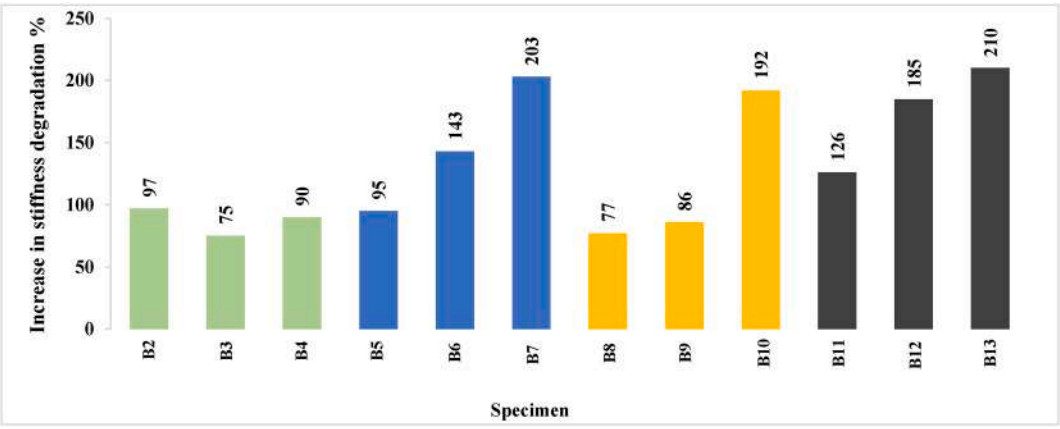

Fig. 13. Influence of fibers on the stiffness degradation of specimens.

Table 7
Different models utilized for predicting the ultimate torsional strength.

Models	Main considerations and equations	Remarks	References
ACI (318M − 14) Model	• According to ACI [35], the calculated torsional strength of the reinforced concrete beams is: $T_{us} = f_{ys}\left(\frac{A_{sw}}{s}\right) 2A_o cot\theta$	• A_{oh} = (b-2c).(h- 2c) • $A_o = 0.85A_{oh}$ • $\theta_t = 45^o$	[35]
GB 50010 Model	• According to GB 50010–2010 [36], the torsional strength for solid beams is: $T_u = T_C + T_R = 0.35 f_t W_t + 1.2\sqrt{\zeta}\frac{f_{yv}A_{st}A_{cor}}{s}$	• A_{cor} = (b-2c).(h- 2c) • u_{cor} = 2[(b-2c)+(h-2c)] • $W_t = \frac{b^2}{6}(3h\text{-}b)$ • $\zeta = \frac{f_y A_{sl} s_t}{f_{yv} A_{st} u_{cor}}$	[36]
Eurocode2 Model	• According to Eurocode2 [37], the ultimate torsion can be calculated as: $T_{us} = f_{ys}(\frac{A_{sw}}{s})2A_k cot\theta_t$ $T_{uL} = f_y(\frac{A_{sl}}{u_k})2A_k tan\theta_t$	• $t_{ef} = \frac{b.h}{2(b+h)}$ • A_k = (b-t_{ef}).(h- t_{ef}) • u_k = 2[(b-t_{ef})+(h-t_{ef})] • $\theta_t = 45^o$	[37]
AS3600 Model	• According to the Australian standard [38], the ultimate torsion can be calculated as: $T_{uc} = J_t(0.3\sqrt{fc'})$ $T_{us} = f_{ys}(\frac{A_{sw}}{s})2A_t cot\theta_t$	• $J_t = 0.4\ X^2Y$ • A_t = (b-2c).(h- 2c) • $\theta_t = 45^o$	[38]
Li Model	• According to Li et al. [39], the torsional strength of UHPC solid beams can be calculated as: $T_u = T_C + T_R = f_t W_t + 1.2\sqrt{\zeta}\frac{f_{yv}A_{st}A_{cor}}{s_t}$	• A_{cor} = (b-2c).(h- 2c) • u_{cor} = 2[(b-2c)+(h-2c)] • $W_t = \frac{b^2}{6}(3h\text{-}b)$ • $\zeta = \frac{f_y A_{sl} s_t}{f_{yv} A_{st} u_{cor}}$	[39]

agreement with the experimental results [$T_{u(exp)}$] and gave good predictions for the ultimate moment as the mean value of [$T_{u(pre)}/T_{u(exp)}$] were 1.053, and 1.049,respectively. In contrast, ACI 318-14 [35], GB 50010 [36], Eurocode2(due to the stirrup's contribution) [37], and AS3600 [38] underestimated the ultimate moment for hybrid fiber reinforced concrete (HFRC) beams as the mean values of [$T_{u(pre)}/T_{u(exp)}$] were 0.31, 0.61, 0.36, and 0.67, respectively.

8.1. Proposed model

As previously described, the main reason for developing this model was that the existing codes' formulas underestimated the torsional strength provided by HFRC tensile capacity. Although the predicted values of Li model [39] were in good agreement with the experimental results, the effect of the hybrid fibers was not taken into consideration. Therefore, this study modified Li formula to take

Table 8
Experimental and predicted ultimate moment results.

Beams	(f_C) (Mpa)	(f_t) (Mpa)	$T_{u(exp)}$ (kN.m)	ACI (318M − 14) [35]		GB 50010 [36]		Eurocode2 [37]				AS3600 [38]		Li Model [39]	
				$T_{u(pre)}$ (kN.m)	$T_{u(pre)}/T_{u(exp)}$	$T_{u(pre)}$ (kN.m)	$T_{u(pre)}/T_{u(exp)}$	$T_{us(pre)}$ (kN.m)	$T_{us(pre)}/T_{u(exp)}$	$T_{uL(pre)}$ (kN.m)	$T_{uL(pre)}/T_{u(exp)}$	$T_{u(pre)}$ (kN.m)	$T_{u(pre)}/T_{u(exp)}$	$T_{u(pre)}$ (kN.m)	$T_{u(pre)}/T_{u(exp)}$
B1	40.20	3.50	14.11	5.26	0.37	9.76	0.69	6.19	0.44	17.88	1.27	11.33	0.80	16.16	1.14
B2	46.30	4.10	18.27	5.26	0.29	10.35	0.57	6.19	0.34	17.88	0.98	11.70	0.64	17.84	0.98
B3	32.85	3.75	13.86	5.26	0.38	10.00	0.72	6.19	0.45	17.88	1.29	10.83	0.78	16.86	1.22
B4	47.80	4.50	21.67	5.26	0.24	10.74	0.50	6.19	0.29	17.88	0.82	11.79	0.54	18.97	0.88
B5	43.00	3.65	13.73	5.26	0.38	9.90	0.72	6.19	0.45	17.88	1.30	11.50	0.84	16.58	1.21
B6	41.50	4.20	17.14	5.26	0.31	10.45	0.61	6.19	0.36	17.88	1.04	11.41	0.67	18.12	1.06
B7	40.60	4.50	17.26	5.26	0.30	10.74	0.62	6.19	0.36	17.88	1.04	11.35	0.66	18.97	1.10
B8	34.50	3.70	13.61	5.26	0.39	9.95	0.73	6.19	0.45	17.88	1.31	10.95	0.80	16.72	1.23
B9	35.20	4.40	17.26	5.26	0.30	10.64	0.62	6.19	0.36	17.88	1.04	11.00	0.64	18.69	1.08
B10	41.10	4.50	18.14	5.26	0.29	10.74	0.59	6.19	0.34	17.88	0.99	11.38	0.63	18.97	1.05
B11	42.00	4.40	19.03	5.26	0.28	10.64	0.56	6.19	0.33	17.88	0.94	11.44	0.60	18.69	0.98
B12	43.80	4.60	21.04	5.26	0.25	10.84	0.52	6.19	0.29	17.88	0.85	11.55	0.55	19.25	0.91
B13	54.10	4.90	23.31	5.26	0.23	11.13	0.48	6.19	0.27	17.88	0.77	12.15	0.52	20.09	0.86
Mean	–	–	–	–	0.31	–	0.61	–	0.36	–	1.05	–	0.67	–	1.05

the effect of hybrid fiber on the ultimate torsion of HFRC beams, as expressed in Eq. (1).

$$T_u = T_C + T_R = f_t\, Cf_t W_t + 1.2\sqrt{\zeta}\,\frac{f_{yv} A_{st} A_{cor}}{s_t} \quad (1)$$

The fiber modified factor (f_r) was developed to incorporate the effect of hybrid fiber dosage, and fiber length as expressed in Eq. (2).

$$f_r = [1 + mA_c\,(V_{SF}L_{SF} + V_{CF}L_{CF} - 0.86\,V_{BF}L_{BF})]^n \quad (2)$$

where T_C and T_R are the torsional strengths derived from the concrete strength and rebar, respectively; C is a coefficient, can be used as 0.79 for high performance concrete or 1 For ultra-high performance concrete; W_t is the section torsional plastic resistance moment, can be calculated as $W_t = \frac{b^2}{6}$ (3h-b); ζ is the strength ratio of longitudinal reinforcement to transverse reinforcement, can be calculated as $\zeta = \frac{f_y A_{sl} s_t}{f_{yv} A_{st} u_{cor}} f_t$ is the tensile strength of concrete; m is a coefficient can be used as 17×10^{-8}; A_c is the beam gross area; V_{SF}, V_{CF}, and V_{BF} are percentages of SF, CF, and BF dosages; L_{SF}, L_{CF}, and L_{BF} are the lengths of SF, CF, and BF, respectively; and n is a coefficient, can be used as 1.5 for single type of fiber or 1.1 for hybrid fibers.

Table 9 presented the predicted ultimate strengths and ratios of predicted-to-experimental ultimate strength [$T_{u(pre)}/T_{u(exp)}$] for the proposed model. It can be observed that the predicted model values [$T_{u(pre)}$] were in good agreement with the experimental results [$T_{u(exp)}$] and gave good predictions for the ultimate moment as the mean value of Tu (pre)/Tu(exp) was 1.00.

In conclusion, Fig. 14, presented a comparison between experimental and theoretical values of the ultimate torsional moment. With comparing all theoretical results to the experimental results we found that ACI 318-14 [35], GB 50010 [36], Eurocode2 (due to the stirrup's contribution) [37], and AS3600 [38] underestimated the ultimate moment for hybrid fiber reinforced concrete (HFRC) beams as the mean values of [$T_{u(pre)}/T_{u(exp)}$] were 0.31, 0.61, 0.36, and 0.67, respectively. On the other hand the proposed model, Li model, and Eurocode2 (due to the longitudinal bars contribution) [37] predicted values were in good agreement with the experimental results and gave good predictions for the ultimate moment as the mean value of [$T_{u(pre)}/T_{u(exp)}$] were 1.00, 1.05, and 1.05, respectively.

9. Conclusion

In this study, the impact of hybrid fiber between CF, BF, and SF on the torsional behavior of reinforced concrete beams. The investigation involved tests on thirteen RC beams under pure torsion load until failure. Specimens were divided into four groups: three groups contain hybrid fiber of (CF and BF), (BF and SF), and (CF and SF) with a varying fiber content of 0.25%, 0.50%, and 0.75% in terms of volume, and the fourth group was control specimens. In the tests, the torsional moment, twisting angle, crack pattern, fracture modes, ductility, and energy absorption of specimens were measured.

The following are brief description of the main conclusions derived from the experimental work performed on HFRC specimens.

1. The use of hybrid fiber enhanced the torsional behavior of RC beams. Therefore, the maximum torsional strength increased by 22.3%, 28.6%, and 65.2% when (0.75% BF and 0.75% CF), (0.75% BF and 0.75% SF) and (0.75% CF and 0.75% SF) added, respectively.
2. All beams showed higher angle of twist than beam without fiber. Especially, adding (0.75% CF and 0.75% SF) to RC beams played a significant role in increasing the angle of twist by 293.44% compared to beam without fibers.
3. The higher modulus of elasticity for CF and SF had a larger influence on increasing cracks propagation throughout the specimens' length and decreasing crack width than other hybrid fibers.
4. Increasing the hybrid fiber content played an important role in bridging micro and macro cracks which made the concrete more ductile. Therefore, we found that the ductility increased by 121.2%, 138.2%, and 130.9% when (0.75% BF and 0.75% CF), (0.75% BF and 0.75% SF) and (0.75% CF and 0.75% SF) added, respectively.

Table 9
Experimental and proposed model ultimate moment results.

Beams	(f_C) (Mpa)	(f_t) (Mpa)	$T_{u(exp)}$ (kN.m)	Proposed model	
				$T_{u(pre)}$ (kN.m)	$T_{u(pre)}/T_{u(exp)}$
B1	40.20	3.50	14.11	14.11	1.00
B2	46.30	4.10	18.27	18.33	1.00
B3	32.85	3.75	13.86	12.88	0.93
B4	47.80	4.50	21.67	21.44	0.99
B5	43.00	3.65	13.73	14.60	1.06
B6	41.50	4.20	17.14	16.03	0.94
B7	40.60	4.50	17.26	16.92	0.98
B8	34.50	3.70	13.61	15.06	1.11
B9	35.20	4.40	17.26	17.32	1.00
B10	41.10	4.50	18.14	18.20	1.00
B11	42.00	4.40	19.03	17.98	0.95
B12	43.80	4.60	21.04	20.50	0.97
B13	54.10	4.90	23.31	23.57	1.00
Mean	–	–	–	–	1.00

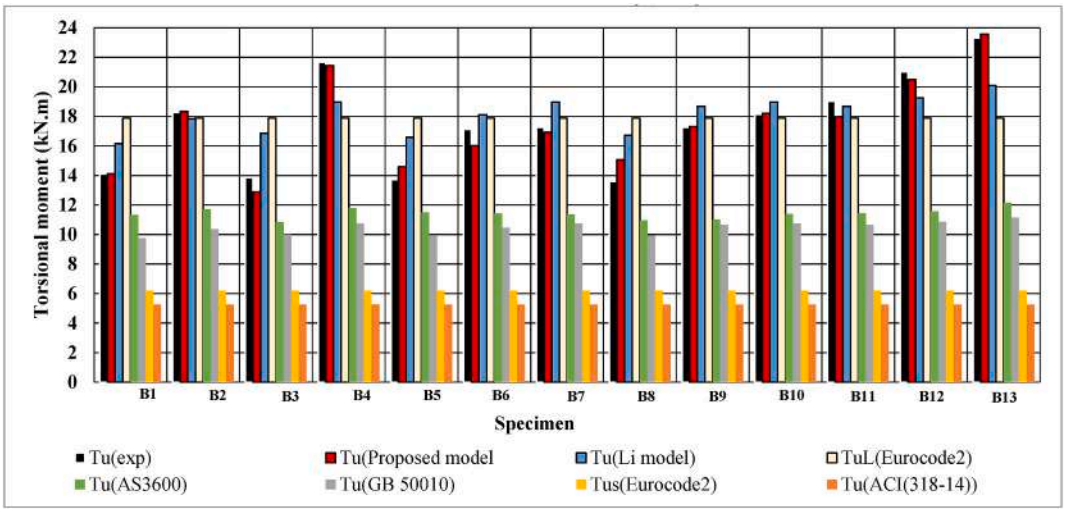

Fig. 14. Comparison between experimental and theoretical values of ultimate torsional moment.

5. The hybrid fiber of CF and SF showed significant improvement in energy absorption compared to other specimens. The energy absorbed increased by 458.3%, 550%, and 641.7% when (0.25% CF and 0.25% SF), (0.50% CF and 0.50% SF) and (0.75% CF and 0.75% SF) added, respectively.
6. The experimental ultimate torsion moments were compared to the predicted values of five models. It was found that ACI 318-14, GB 50010, Eurocode2, and AS3600 underestimated the ultimate moment. While Li models' predicted values were in good agreement with the experimental results.
7. Proposed model was developed to predict the influence of hybrid fiber on the ultimate torsion of HFRC beams. The fiber-modified factor (f_r) has been added to the proposed equation to incorporate the effect of hybrid fiber dosage, and fiber length. The predicted model values were in good agreement with the experimental results and gave good predictions for the ultimate moment as the mean value of Tu (pre)/Tu(exp) was 1.00.

10. Recommendations

From the results of this study, we recommend a combination of at least hybrid fibers (0.75% CF and 0.75% SF) to achieve adequate torsional behavior of hybrid fiber reinforced concrete beams. This combination increased significantly the maximum torsional moment and improved the ductility of HFRC beams. Therefore, it is recommended to investigate the effect of increasing carbon fiber content and adding more than two fibers together to study the influence of those combinations on the torsional behavior.

Authors statement

Mohamed Said.

Prof. Dr. Mohamed Said Abdel-Ghaffar Professor of Reinforced Concrete Structures Faculty of Engineering (Shoubra) Benha University. Email: mohamed.abdelghaffar@feng.bu.edu.eg.

Ahmed Salah.

Dr. Ahmed Mohamed Salah-Eldin Ahmed Salem Assistant Professor Faculty of Engineering (Shoubra) Benha University. Email: ahmed.salaheldin@feng.bu.edu.eg.

Abeer Erfan.

Dr. Abeer Medhat Mohamed Erfan Associate Professor of Concrete Structures Faculty of Engineering (Shoubra) Benha University Email: abir.arfan@feng.bu.edu.eg.

Ahmed Esam.

Eng. Ahmed Esam Salem Demonstrator in Department of civil engineering, Higher Institute of Engineering, Shorouk City, Cairo, Egypt Email: ahmed.esam@sha.edu.eg.

Declaration of competing interest

The authors declare that they have no known competing financial interests or personal relationships that could have appeared to influence the work reported in this paper.

Data availability

The authors do not have permission to share data.

References

[1] R. Liu, H. Li, Q. Jiang, X. Meng, Experimental investigation on flexural properties of directional steel fiber reinforced rubberized concrete, Structures 27 (2020) 1660–1669, https://doi.org/10.1016/j.istruc.2020.08.007.

[2] J. Ran, T. Li, D. Chen, L. Shang, W. Li, Q. Zhu, Mechanical properties of concrete reinforced with corrugated steel fiber under uniaxial compression and tension, Structures 34 (2021) 1890–1902, https://doi.org/10.1016/j.istruc.2021.08.135.

[3] J. Zhou, W. Shen, S. Wang, Experimental study on torsional behavior of FRC and ECC beams reinforced with GFRP bars, Construct. Build. Mater. 152 (2017) 74–81, https://doi.org/10.1016/j.conbuildmat.2017.06.131.

[4] S. Gali, K.V.L. Subramaniam, Investigation of the dilatant behavior of cracks in the shear response of steel fiber reinforced concrete beams, Eng. Struct. 152 (2017) 832–842, https://doi.org/10.1016/j.engstruct.2017.09.050.

[5] A. Hadhood, M.G. Gouda, M.H. Agamy, Torsion in concrete beams reinforced with GFRP spirals, Eng. Struct. 206 (2020), 110174, https://doi.org/10.1016/j.engstruct.2020.110174.

[6] S.B. Kandekar, R.S. Talikoti, Torsional behaviour of reinforced concrete beam wrapped with aramid fiber, J. King Saud Univ. - Eng. Sci. 31 (2019) 340–344, https://doi.org/10.1016/j.jksues.2018.02.001.

[7] M.Y. Alabdulhady, L.H. Sneed, A study of the effect of fiber orientation on the torsional behavior of RC beams strengthened with PBO-FRCM composite, Construct. Build. Mater. 166 (2018) 839–854, https://doi.org/10.1016/j.conbuildmat.2018.02.004.

[8] M.Y. Alabdulhady, L.H. Sneed, O.I. Abdelkarim, M.A. Elgawady, Finite element study on the behavior of RC beams strengthened with PBO-FRCM composite under torsion, Compos. Struct. 179 (2017) 326–339, https://doi.org/10.1016/j.compstruct.2017.07.079.

[9] J. Zhou, W. Shen, S. Wang, Experimental study on torsional behavior of FRC and ECC beams reinforced with GFRP bars, Construct. Build. Mater. 152 (2017) 74–81, https://doi.org/10.1016/j.conbuildmat.2017.06.131.

[10] T. Jasim, B.H.A. Bakar, N.M. Bunnori, Torsional improvement of reinforced concrete beams using ultra high-performance fiber reinforced concrete (UHPFC) jackets – experimental study, Construct. Build. Mater. 106 (2016) 533–542, https://doi.org/10.1016/j.conbuildmat.2015.12.160.

[11] G. Charan, T.D.G. Rao, C.B.K. Rao, Case Studies in Construction Materials Torsional behaviour of reinforced concrete beams with ferrocement U-jacketing — experimental study, Case Stud. Constr. Mater. 4 (2016) 15–31, https://doi.org/10.1016/j.cscm.2015.10.003.

[12] A. Karimipour, J. de Brito, M. Ghalehnovi, O. Gencel, Torsional behaviour of rectangular high-performance fibre-reinforced concrete beams, Structures 35 (2022) 511–519, https://doi.org/10.1016/j.istruc.2021.11.037.

[13] M.A. Hadi, S.D. Mohammed, Materials Today : proceedings Improving torsional – flexural resistance of concrete beams reinforced by hooked and straight steel fibers, Mater. Today Proc. 42 (2021) 3072–3082, https://doi.org/10.1016/j.matpr.2020.12.1046.

[14] R.F. Hassan, M.H. Jaber, N.H. Al-salim, H.H. Hussein, Experimental research on torsional strength of synthetic/steel fi ber- reinforced hollow concrete beam, Eng. Struct. 220 (2020), 110948, https://doi.org/10.1016/j.engstruct.2020.110948.

[15] K.J.N.S. Nitesh, S.V. Rao, P.R. Kumar, An experimental investigation on torsional behaviour of recycled aggregate based steel fi ber reinforced self compacting concrete, J. Build. Eng. 22 (2019) 242–251, https://doi.org/10.1016/j.jobe.2018.12.011.

[16] S.P. Patil, K.K. Sangle, Tests of steel fi bre reinforced concrete beams under predominant torsion, J. Build. Eng. 6 (2016) 157–162, https://doi.org/10.1016/j.jobe.2016.02.004.

[17] T. Senthuran, S.S. A, Experimental study on torsional behaviour of crimped steel fiber, Reinforced Beam 6 (2016) 3950–3953, https://doi.org/10.4010/2016.911.

[18] S.P. Yap, K.R. Khaw, U.J. Alengaram, M.Z. Jumaat, Effect of fibre aspect ratio on the torsional behaviour of steel fibre-reinforced normal weight concrete and lightweight concrete, Eng. Struct. 101 (2015) 24–33, https://doi.org/10.1016/j.engstruct.2015.07.007.

[19] J.J. Zeng, B.Z. Pan, T.H. Fan, Y. Zhuge, F. Liu, L.J. Li, Shear behavior of FRP-UHPC tubular beams, Compos. Struct. 307 (2023), 116576, https://doi.org/10.1016/j.compstruct.2022.116576.

[20] J.J. Zeng, W. Bin Zeng, Y.Y. Ye, J.J. Liao, Y. Zhuge, T.H. Fan, Flexural behavior of FRP grid reinforced ultra-high-performance concrete composite plates with different types of fibers, Eng. Struct. 272 (2022) 24–26, https://doi.org/10.1016/j.engstruct.2022.115020.

[21] X. Sun, Z. Gao, P. Cao, C. Zhou, Mechanical properties tests and multiscale numerical simulations for basalt fiber reinforced concrete, Construct. Build. Mater. 202 (2019) 58–72, https://doi.org/10.1016/j.conbuildmat.2019.01.018.

[22] W. Alnahhal, O. Aljidda, Flexural behavior of basalt fiber reinforced concrete beams with recycled concrete coarse aggregates, Construct. Build. Mater. 169 (2018) 165–178, https://doi.org/10.1016/j.conbuildmat.2018.02.135.

[23] Z. Guo, C. Zhuang, Z. Li, Y. Chen, Mechanical properties of carbon fi ber reinforced concrete (CFRC) after exposure to high temperatures, Compos. Struct. 256 (2021), 113072, https://doi.org/10.1016/j.compstruct.2020.113072.

[24] Z. Wang, G. Ma, Z. Ma, Y. Zhang, Flexural behavior of carbon fiber-reinforced concrete beams under impact loading, Cem. Concr. Compos. 118 (2021), 103910, https://doi.org/10.1016/j.cemconcomp.2020.103910.

[25] I.G. Shaaban, M. Said, S.U. Khan, M. Eissa, K. Elrashidy, Experimental and theoretical behaviour of reinforced concrete beams containing hybrid fibres, Structures 32 (2021) 2143–2160, https://doi.org/10.1016/j.istruc.2021.04.021.

[26] P. Saravanakumar, M. Sivakamidevi, K. Meena, S.P. Yamini, Materials Today : proceedings an experimental study on hybrid fiber reinforced concrete beams subjected to torsion, Mater. Today Proc. 45 (2021) 6818–6821, https://doi.org/10.1016/j.matpr.2020.12.1003.

[27] F. Shi, T.M. Pham, H. Hao, Y. Hao, Post-cracking behaviour of basalt and macro polypropylene hybrid fibre reinforced concrete with different compressive strengths, Construct. Build. Mater. 262 (2020), 120108, https://doi.org/10.1016/j.conbuildmat.2020.120108.

[28] M. Khan, M. Cao, M. Ali, Cracking behaviour and constitutive modelling of hybrid fibre reinforced concrete, J. Build. Eng. 30 (2020), 101272, https://doi.org/10.1016/j.jobe.2020.101272.

[29] B. Li, Y. Chi, L. Xu, Y. Shi, C. Li, Experimental investigation on the flexural behavior of steel-polypropylene hybrid fiber reinforced concrete, Construct. Build. Mater. 191 (2018) 80–94, https://doi.org/10.1016/j.conbuildmat.2018.09.202.

[30] P. Smarzewski, Hybrid fibres as shear reinforcement in high-performance concrete beams with and without openings, Appl. Sci. (2018), https://doi.org/10.3390/app8112070.

[31] P. Smarzewski, Analysis of failure mechanics in hybrid fibre-reinforced high-performance concrete deep beams with and without openings, Materials (Basel) (2019), https://doi.org/10.3390/ma12010101.

[32] G. Asok, S. George, Investigation on hybrid concrete using steel and polypropylene fiber, New Technol. Res. (2016) 61–64.

[33] Y. Zhang, L.K. Korkiala-Tanttu, M. Borén, Assessment for sustainable use of quarry fines as pavement construction materials: Part II-stabilization and characterization of quarry fine materials, Materials (Basel) 12 (2019), https://doi.org/10.3390/ma12152450.

[34] A.N. Hanoon, A.A. Abdulhameed, H.A. Abdulhameed, S.K. Mohaisen, Energy absorption evaluation of CFRP-strengthened two-spans reinforced concrete beams under pure torsion, Civ. Eng. J. 5 (2019) 2007–2018, https://doi.org/10.28991/cej-2019-03091389.

[35] A.C.I. ACI, Building Code Requirements for Structural Concrete, 2014.

[36] GB 50010-2010, Code for design of concrete structures, in: Beijing, Gen. Adm. Qual. Supervision, Insp. Quar. People's Repub. China Stand. Adm. People's Repub. China [in Chinese]Administration Qual, 2015. Supervision, Insp.

[37] Eurocode 2, Design of Concrete Structures - Part, vol. 1, 2002.

[38] C.S. Committee BD-002, AS 3600 - Concrete Structures, 2001.

[39] C. Li, J. Zhou, L. Ke, S. Yu, H. Li, Failure mechanisms and loading capacity prediction for rectangular UHPC beams under pure torsion, Eng. Struct. 264 (2022), https://doi.org/10.1016/j.engstruct.2022.114426.

Notation

PC: plain concrete
RC: reinforced concrete
HRWR: high range water reducer
dia: diameter
μ: ductility ratio
PBO: phenylene Benzobis Oxazole
ECC: engineered cementitious composite
$CaCO_3$: Calcium Carbonate
LVDT: linear variable differential transformer
↓: diameter of rebars
FRCM: fiber reinforced cementitious matrix
Ku: ultimate stiffness
A_o: the area enclosed by the shear flow path
A_{oh}: the area enclosed by the center of stirrups
A_{sw}: the cross-sectional area of stirrups
A_k: the area enclosed by the centerlines of the effective wall thickness
A_{st}: is the cross-sectional area of stirrups
A_{sl}: the total area of longitudinal steel bar
A_{cor}: the core area closed by one stirrup
A_k: the area enclosed by the centerlines of the effective wall thickness
A_t: is the area enclosed by the centerlines of longitudinal bars
T_C: the torsional strengths derived from the concrete strength
T_R: the torsional strengths derived from the rebar strength
T_u: the ultimate torsional strength
T_f: the torsional strengths at failure
T_{uc}: the ultimate strength in pure torsion for a beam without closed ties
T_{us}: the ultimate torsion due to the stirrup's contribution
T_{uL}: the ultimate torsion due to the longitudinal bars contribution
J_t: the torsional rigidity of the cross-section area
h: the height of the tested beam
X: the width of the beam
FRC: fiber reinforced concrete
HFRC: hybrid fiber reinforced concrete
CF: carbon fiber
SF: steel fiber
BF: basalt fiber
PVA: polyvinyl alcohol
PPF: polypropylene fiber
PP: polypropylene
GFRP: glass fiber reinforced polymer
UHPC: ultra-high-performance concrete
CFRC: carbon fiber reinforced concrete
Ki: Initial stiffness
S: the spacing of stirrups (c/c)
S_t: the spacing of stirrups (c/c)
u_{cor}: the perimeter of the center line of shear flow
u_k: the perimeter of the area A_k
f_{ys}: the yield strength of
f_{yv}: the tensile strength of stirrups
f_y: the yield strength of the longitudinal steel bar
f_c': the cylinder compressive strength of concrete at (28) days
f_t: the tensile strength of concrete
θ_t: the crack angle
θ_f: the failure torsional angle
θ_y: the angle corresponding to the yield point
W_t: the section torsional plastic resistance moment
ζ: the strength ratio of longitudinal reinforcement to transverse reinforcement
b: the width of the tested beam
t_{ef}: the effective wall thickness
c: the concrete cover
Y: the height of the beam